

## Ion beam synthesis of cubic FeSi<sub>2</sub>

J. Desimoni, H. Bernas, M. Behar, X. W. Lin, J. Washburn, and Z. Liliental-Weber

Citation: *Applied Physics Letters* **62**, 306 (1993); doi: 10.1063/1.108969

View online: <http://dx.doi.org/10.1063/1.108969>

View Table of Contents: <http://scitation.aip.org/content/aip/journal/apl/62/3?ver=pdfcov>

Published by the AIP Publishing

---

### Articles you may be interested in

[Endotaxially stabilized B<sub>2</sub>-FeSi nanodots in Si \(100\) via ion beam co-sputtering](#)

*Appl. Phys. Lett.* **104**, 161903 (2014); 10.1063/1.4872315

[Photoreflectance study of ion beam synthesized  \$\beta\$ -FeSi<sub>2</sub>](#)

*J. Appl. Phys.* **91**, 1219 (2002); 10.1063/1.1428792

[Raman investigation of ion beam synthesized  \$\beta\$ -FeSi<sub>2</sub>](#)

*J. Appl. Phys.* **89**, 965 (2001); 10.1063/1.1326473

[Metastable  \$\gamma\$  phase in ion beam synthesized FeSi<sub>2</sub>](#)

*Appl. Phys. Lett.* **68**, 1784 (1996); 10.1063/1.116666

[Low-temperature ion-induced epitaxial growth of  \$\alpha\$ -FeSi<sub>2</sub> and cubic FeSi<sub>2</sub> in Si](#)

*Appl. Phys. Lett.* **63**, 105 (1993); 10.1063/1.109727

---



**NEW Special Topic Sections**

**NOW ONLINE**  
Lithium Niobate Properties and Applications:  
Reviews of Emerging Trends

**AIP** | Applied Physics  
Reviews

# Ion beam synthesis of cubic FeSi<sub>2</sub>

J. Desimoni,<sup>a)</sup> H. Bernas, and M. Behar<sup>b)</sup>

Centre de Spectrométrie Nucléaire et Spectrométrie de Masse, Bât. 108, 91405 Orsay Campus, France

X. W. Lin, J. Washburn, and Z. Liliental-Weber

Lawrence Berkeley Laboratory, Berkeley, California 94720

(Received 20 May 1992; accepted for publication 28 October 1992)

Cubic FeSi<sub>2</sub> precipitates were synthesized in Si (100) by room-temperature Fe ion implantation followed by Si 500 keV ion beam induced epitaxial crystallization at 320 °C. High resolution electron microscopy and Rutherford backscattering/channeling techniques show that the cubic precipitates occur in both aligned (A) and twinned (B) types with a lattice parameter very similar to that of the Si (100) matrix.

Because of possible applications in silicon technology, considerable work has been performed in recent years on the synthesis and properties of iron disilicide. The two known stable phases<sup>1-3</sup> are the tetragonal (metallic)  $\alpha$ -FeSi<sub>2</sub> phase, and the orthorhombic (semiconducting)  $\beta$ -FeSi<sub>2</sub>, which grows epitaxially on Si (111) and is stable up to 940 °C. Recently a metastable (metallic<sup>4</sup>) cubic FeSi<sub>2</sub> phase, with a lattice parameter similar to that of Si, was obtained by different forms of solid phase epitaxy<sup>4,5</sup> at temperatures below 400 °C on a Si (111) substrate. This phase converts to  $\beta$ -FeSi<sub>2</sub> when the layer thickness exceeds a critical value (typically 0.6–30 nm).

Since the cubic phase is metastable, the possibility of forming it by nonequilibrium techniques such as pulsed laser annealing or ion beam treatments warrants study. Pulsed laser irradiation of an SPE  $\beta$ -FeSi<sub>2</sub> layer grown on a Si (111) substrate<sup>6</sup> produced a 30 nm thick cubic phase epitaxial layer in B-type (twinned). The aim of the present work was to determine whether it is possible to form cubic FeSi<sub>2</sub> using Fe implantation and subsequent ion beam induced epitaxial crystallization (IBIEC) of the Si host. We show that isolated epitaxial cubic FeSi<sub>2</sub> precipitates can be formed in this way.

Si(100) wafers (*p*-type, 1  $\Omega$  cm) were room-temperature implanted with Fe at energies between 50 and 180 keV and fluences between  $1 \times 10^{16}$  and  $4 \times 10^{16}$  Fe cm<sup>-2</sup> (corresponding to peak Fe concentrations between ca. 4–7 at. %). Implantation current densities were below 1  $\mu$ A cm<sup>-2</sup> in order to minimize sample heating. Channelled implantation was avoided by tilting samples by 7° with respect to the ion beam. IBIEC was carried out at 320 °C with the ARAMIS high-energy implanter<sup>8</sup> using a 500 keV Si beam (current density ca. 1  $\mu$ A cm<sup>2</sup>, total fluences between  $4 \times 10^{16}$  and  $1 \times 10^{17}$  Si cm<sup>-2</sup>). The samples were analyzed *in situ* by Rutherford backscattering and channeling (RBS/C) at 165° scattering angle using 1.2 MeV He ions. The near-surface Fe distribution was studied by RBS at a scattering angle of 83°. Transmission electron microscopy (TEM), selected area diffraction (SAD), and high resolution electron microscopy (HREM) were per-

formed at Lawrence Berkeley Laboratory.

Figure 1 displays the random and channelled RBS spectra of a sample implanted at 50 keV with  $1 \times 10^{16}$  Fe cm<sup>-2</sup>. The Si wafer was amorphized over 100 nm. Figure 2 shows that after the subsequent 500 keV Si irradiation at 320 °C, the entire amorphous layer was recrystallized, the minimum backscattering yield on subsurface Si being  $\chi_{\min}=0.12$ . Some channeling was observed in the Fe part of the spectrum ( $\chi_{\min}=0.73$ ). The corresponding grazing RBS experiment (not shown here) showed that about 10% of the implanted Fe atoms were transported to the surface as a consequence of the IBIEC process.

Shown in Fig. 3(a) is a TEM bright-field image of an IBIEC-processed sample viewed along Si [110]. This sample was implanted at two different energies (180 and 100 keV) in order to obtain a reasonably uniform Fe concentration of 7 at. %. It displays a layered structure with (i) a 150 nm thick layer just below the surface, (ii) a dark-contrasted layer, 600 nm thick, sandwiched between the latter, and (iii) a relatively unperturbed Si. The middle of the dark contrasted layer corresponds to the projected range of 500 keV Si ( $R_p=750$  nm). In spite of the

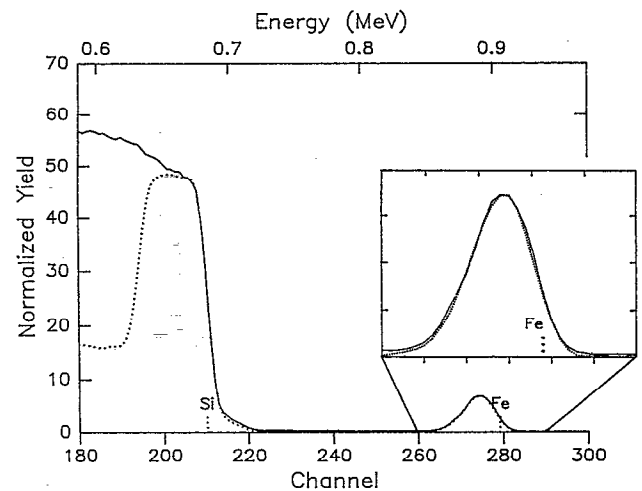


FIG. 1. Random (full line) and [100] channelled RBS spectra (dots) of a Si (100) sample implanted with 50 keV Fe at a fluence of  $1 \times 10^{16}$  at cm<sup>-2</sup>. The amorphous layer is 100 nm thick. The inset shows the random and channeling spectra corresponding to the Fe profile.

<sup>a)</sup>On leave from Departamento de Física, Facultad de Ciencias Exactas, U.N.L.P., under a fellowship of CONICET, Argentina.

<sup>b)</sup>On leave from Instituto de Física, U.F.R.G.S. Porto Alegre, Brazil.

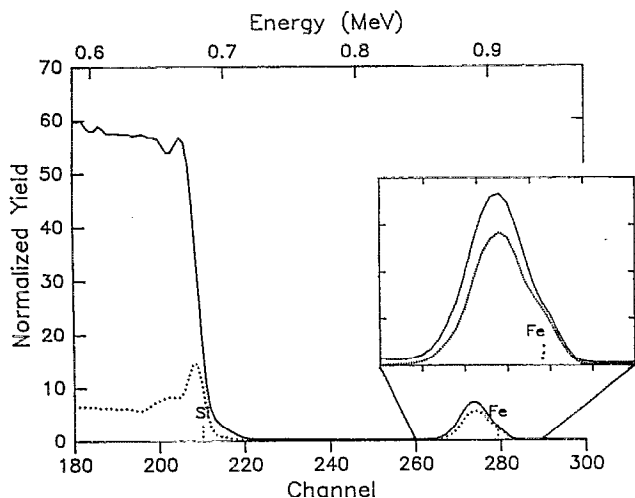


FIG. 2. Random (full line) and channeled RBS spectra (dots) of the same sample displayed in Fig. 1, after a  $4 \times 10^{16}$  at  $\text{cm}^{-2}$  Si irradiation at 320 °C. The Fe profile shows a partial degree of alignment—see inset—and Si substrate has completely recrystallized.

irradiation-induced damage, the structure of this layer remains crystalline, as indicated by its SAD pattern [Fig. 3(c)] which corresponds to the Si [110] zone axis.

Figure 3(b) is a SAD pattern taken from the surface layer where the most intense spots are indexed as reflections from the Si [110] zone axis. A regular array of weak spots is superimposed on the Si spots. These spots can be interpreted as reflections from a cubic  $\text{FeSi}_2$  phase whose lattice parameter is almost identical to that of the Si matrix. Figure 4 shows HREM images of near-surface  $\text{FeSi}_2$  precipitates with a diameter ca. 5 nm. Two types of  $\text{FeSi}_2$  precipitates can be recognized. Type A [Fig. 4(c)], corre-

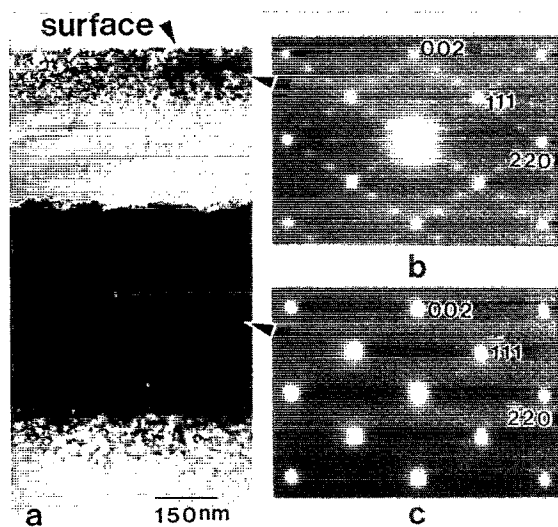


FIG. 3. (a) A TEM micrograph showing the cross section of an IBIEC-processed Fe-implanted Si. (b) An SAD pattern taken from the surface layer. The most intense spots are indexed as reflections from the Si [100] zone axis and the weak ones are due to the B-type cubic  $\text{FeSi}_2$  precipitates [see Fig. 4(b)] combined with the double diffraction effect. (c) A SAD pattern from dark-contrasted layer showing reflections from the Si [100] zone axis.

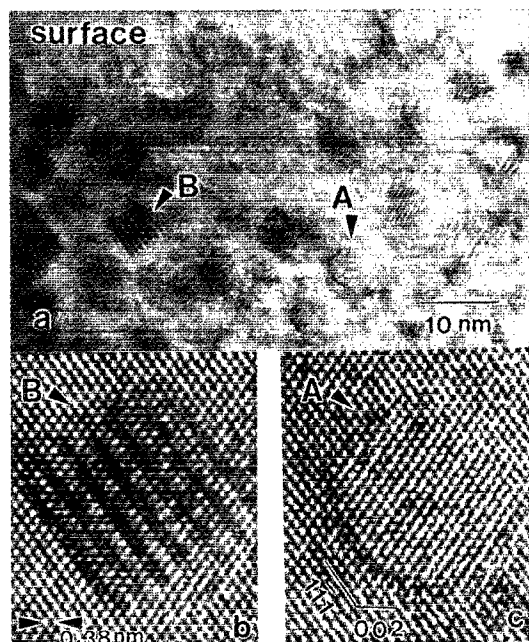


FIG. 4. (a) An HREM image of the surface layer viewed along Si [100]. Arrows A and B indicate two types of precipitates that are formed epitaxially in the Si matrix. (b) An HREM image of a B-type precipitate seen at a higher magnification. (c) An HREM image of an A-type precipitate seen at a higher magnification.

sponds to precipitates formed epitaxially in the Si matrix with a *fully aligned orientation relationship to the Si matrix*. Type B [Fig. 4(b)] corresponds to precipitates that are rotated  $180^\circ$  about [111] of Type A, i.e., twinned relative to Type A. Thus, the weak spots in Fig. 3(b) are due to reflections from the B-type precipitates, together with the double diffraction effect, whereas the reflections from the A-type  $\text{FeSi}_2$  precipitates cannot be seen in Fig. 3(b) because they overlap with the spots of the Si [110] zone axis.

Note that in previous work<sup>5,6</sup> only B-type orientation was observed, whereas here both A- and B-type precipitates occur. Preliminary results show that decreasing the Fe concentration increases the proportion of A-type. Finally, in Ref. 6 the stability of the continuous cubic  $\text{FeSi}_2$  layer was checked up to 300 °C; post-irradiation vacuum furnace annealing performed at 520 °C did not affect the structure of the cubic phase precipitates in our case.

To our knowledge, this is the first report that aligned cubic  $\text{FeSi}_2$  precipitates can be formed by an ion beam technique.

The technical support of the Semiramis Group at Orsay is acknowledged, as well as W. Swider for help in TEM specimen preparation. Discussions with J. Derrien and J. Chevrier were essential. The microscopy was performed with the facilities of the National Center for Electron Microscopy funded by the U.S. Department of Energy under Contract No. DE-AC03-76SF00098.

- J. E. Mahan, K. M. Geib, G. Y. Robinson, R. G. Long, Y. Xinghua, G. Bai, M. A. Nicolet, and M. Nathan, *Appl. Phys. Lett.* **56**, 2126 (1990).
- K. Rademacher, S. Mantl, Ch. Dicker, and H. Luth, *Appl. Phys. Lett.* **59**, 2145 (1991).
- D. J. Oostra, D. E. W. Vandenhoude, C. W. T. Bulle-Lieuwma, and E.

P. Naburgh, *Appl. Phys. Lett.* **59**, 1737 (1991).

<sup>4</sup>J. Chevrier, V. Le Than, S. Nitzche, and J. Derrien, *Appl. Surf. Sci.* **56-58**, 438 (1992); V. Le Than, J. Chevrier, and J. Derrien, *Phys. Rev. B* (to be published).

<sup>5</sup>N. Onda, J. Henz, E. Muller, K. A. Mader, and H. von Kanel, *Appl. Surf. Sci.* **56-58**, 421 (1992).

<sup>6</sup>M. G. Grimaldi, P. Baeri, C. Spinella, and S. Lagomarsino, *Appl. Phys. Lett.* **60**, 1132 (1992).

<sup>7</sup>F. Priolo and E. Rimini, *Mater. Sci. Rep.* **5**, 319 (1990).

<sup>8</sup>H. Bernas, J. Chaumont, E. Cottreau, R. Meunier, A. Traverse, C. Clerc, O. Kaitasov, F. Lalu, D. Le Du, G. Moroy, and M. Salomé, *Nucl. Instrum. Methods* **62**, 416 (1992).